phys. stat. sol. (b) **227**, No. 2, 365–379 (2001)

Editor's Choice

Charged Magnetoexcitons in Two Dimensions: Isolated X^- and Many-Electron Effects

A. B. DZYUBENKO[1]), H. A. NICKEL, T. YEO, B. D. MCCOMBE, and A. PETROU

Department of Physics, SUNY at Buffalo, Buffalo, NY 14260, USA

(Received June 27, 2001; in revised form July 2, 2001; accepted July 2, 2001)

Subject classification: 71.35.Ji; 73.20.Mf; 73.21.Fg; S7.12

The states of charged magnetoexcitons in two-dimensional systems are considered. Exact optical selection rules for intra- and inter-band processes are discussed. The effect of excess electrons on internal transitions of negatively charged excitons X^- in quantum wells is studied experimentally and theoretically. An experimentally observed blue-shift with excess electron density is explained in terms of collective excitations, magnetoplasmons bound to a valence band hole.

1. Introduction

The existence of three-particle mobile semiconductor hydrogenic complexes, negatively (X^-) and positively (X^+) charged excitons, or trions, was predicted many years ago [1]. These species are the bound states of two electrons and one hole (2e–h) and one electron and two holes (e–2h), respectively. Reduction of the dimensionality enhances the binding of the X^- and X^+ considerably [2–4]. Experimentally, X^- has been identified in magneto-optical spectra of a low-density quasi-two-dimensional electron gas (2DEG) in quantum wells (QWs) [5]. The observation in magnetic fields B of spin-singlet and spin-triplet X^- and X^+ charged excitons in QWs has been subsequently reported by many groups [6–13]. The bulk of the experimental work to date has been concentrated on interband magneto-optics. More recently, intraband internal transitions of charged excitons have been studied [14]. Theoretically, the behavior of X^- at high B (charged magnetoexcitons), has been studied in the strictly-2D geometry [15], in realistic QWs [16, 17], in a confining potential of a donor ion [18] and a quantum dot [19], and in a spherical geometry [20, 21][2]). The binding of X^- at low magnetic fields has also been studied [23, 24].

The trions, X^- and X^+, are often considered to be semiconductor analogs of the negative, H^-, and positive, H_2^+, hydrogen ions. This analogy, however, is not complete. Indeed, the hydrogen ions are usually treated in the infinite proton mass approximation [25] and more closely resemble *localized* semiconductor complexes, such as the two-electron negative donor ion, D^-. The latter has been extensively studied in 2D systems

[1]) Tel.: +1–(716)–645–3926; Fax: +1–(716)–645–2507; e-mail: ad26@acsu.buffalo.edu (on leave from General Physics Institute, RAS, 117942 Moscow, Russia).

[2]) In Haldane's spherical geometry [22] in addition to the axial symmetry, there is the spherical rotational symmetry. The latter is some analogue of the translational symmetry on the plane. Because of the finite size effects (a finite degeneracy of LLs), the e–h spectra are completely discrete in the spherical geometry in B (see [20, 21]) and, in this respect, are qualitatively different from those on a plane.

 0370-1972/01/22710-0365 $ 17.50+.50/0

in B (see, e.g. [26–30], and references therein). In the case of X^-, there are some fundamental differences in the basic physics, which derive from the *free motion* of the complex. For charged systems in B components of the magnetic translation operator do not commute, $[\hat{K}_x, \hat{K}_y] \neq 0$, although both commute with the Hamiltonian, $[\hat{\mathbf{K}}, H] = 0$. Therefore, translations form a non-commutative group and the corresponding dynamical symmetry is often called *magnetic translational symmetry* (see [31–33], and references therein). It has been used in the study of the motion of atomic ions in magnetic fields [34]. This symmetry and the corresponding exact optical selection rule for charged magnetoexcitons (MXs) have been identified only recently [35, 36].

The aim of this paper is twofold. First, we present an overview of the underlying symmetries (Section 2) and exact optical selection rules (Section 3) for charged e–h complexes in magnetic fields; eigenspectra of the strictly 2D X^- states in several lowest Landau levels (LLs) are presented in Section 4. Second, results of experimental and theoretical studies of the effect of excess electrons on internal X^- transitions are given (Section 5).

2. Charged Electron–Hole Complexes in a Magnetic Field

We consider in the effective mass approximation charged e–h complexes in a semiconductor with a simple valence band in a magnetic field; the exchange e–h interaction is neglected. General symmetry properties are illustrated through the example of a three-particle negatively charged exciton X^-. Analogous considerations apply to other charged e–h complexes. The Hamiltonian describing the 2D charged exciton X^- in a perpendicular magnetic field $\mathbf{B} = (0, 0, B)$ is given by

$$H = H_0 + H_{\text{int}}\,, \tag{1}$$

where the free-particle part is

$$H_0 = \sum_{i=1,2} \frac{\hat{\boldsymbol{\pi}}_{ei}^2}{2m_{\text{e}}} + \frac{\hat{\boldsymbol{\pi}}_{\text{h}}^2}{2m_{\text{h}}}\,, \tag{2}$$

and $\hat{\boldsymbol{\pi}}_j = -i\hbar\nabla_j - \dfrac{e_j}{c}\,\mathbf{A}(\mathbf{r}_j)$ are kinematic momentum operators. The interaction Hamiltonian is

$$H_{\text{int}} = U_{\text{ee}}(|\mathbf{r}_1 - \mathbf{r}_2|) + \sum_{i=1,2} U_{\text{eh}}(|\mathbf{r}_i - \mathbf{r}_{\text{h}}|)\,. \tag{3}$$

In concrete calculations the Coulomb interactions $U_{\text{ee}} = -U_{\text{eh}} = e^2/\epsilon r$ are considered, otherwise particular forms of the interaction potentials can be rather arbitrary. We will use the symmetric gauge $\mathbf{A} = \mathbf{B} \times \mathbf{r}/2$. The exact eigenstates of (1) can be labeled as [36]

$$|\Psi_{k\,M_z\,S_{\text{e}}S_{\text{h}}\nu}\rangle\,. \tag{4}$$

Here M_z is the total angular momentum projection, an eigenvalue of $\hat{L}_z = \sum_j (\mathbf{r}_j \times -i\hbar\nabla_j)_z$. The total spin of two electrons can be either $S_{\text{e}} = 0$ (singlet states) or $S_{\text{e}} = 1$ (triplet states); S_{h} denotes the spin state of the hole. The discrete quantum number $k = 0, 1, \ldots$ is associated with magnetic translations. Indeed, the Hamiltonian (1) commutes [31, 32, 34–37] with the operator of the magnetic translations, $[\hat{\mathbf{K}}, H] = 0$. Here $\hat{\mathbf{K}} = \sum_j \hat{\mathbf{K}}_j$, and $\hat{\mathbf{K}}_j = \hat{\boldsymbol{\pi}}_j - \dfrac{e_j}{c}\,\mathbf{r}_j \times \mathbf{B}$ are the generators of magnetic translations of individual particles. In the symmetric gauge, $\hat{\mathbf{K}}_j(\mathbf{B}) = \hat{\boldsymbol{\pi}}_j(-\mathbf{B})$. Indepen-

dent of the gauge, $\hat{\mathbf{K}}_j$ and $\hat{\boldsymbol{\pi}}_j$ commute: $[\hat{K}_{jp}, \hat{\pi}_{jq}] = 0$, $p, q = x, y$. Noting that $[\hat{K}_x, \hat{K}_y] = -i\,\dfrac{\hbar B}{c}\,Q$, where the total charge $Q \equiv \sum_j e_j = -e$ for the X^-, and introducing the dimensionless operator

$$\hat{\mathbf{k}} = \left(\frac{c}{\hbar B\,|Q|}\right)^{1/2} \hat{\mathbf{K}} \tag{5}$$

with canonically conjugate components, one obtains the lowering and raising Bose ladder operators for the whole system [32, 34–37]

$$\hat{k}_\pm = \pm\frac{i}{\sqrt{2}}\,(\hat{k}_x \pm i\hat{k}_y)\,, \qquad [\hat{k}_+, \hat{k}_-] = -\frac{Q}{|Q|} = 1\,. \tag{6}$$

Therefore, $\hat{\mathbf{k}}^2 = \hat{k}_+\hat{k}_- + \hat{k}_-\hat{k}_+$ has the discrete oscillator eigenvalues $2k + 1$, $k = 0, 1, \ldots$. Because of the non-commutativity and hermiticity of $\hat{K}_x$ and $\hat{K}_y$, there is a macroscopic (Landau) degeneracy in k. This degeneracy is quite natural because physically k describes the center-of-rotation of the charged complex in B. Finally, ν in (4) is the principal quantum number. It can be discrete (bound states) or continuous (unbound states forming a continuum); see below. Each ν-th family of macroscopically degenerate states starts with its *Parent State* that has $k = 0$ – *the center of orbit is the origin* – and has the largest (for $Q < 0$) possible M_z in the family. The value of M_z for the PS is determined by particulars of interactions and cannot be established from simple considerations. Daughter states in the ν-th family, $|\Psi^{(\mathrm{D})}_{kM_z - kS_eS_h\nu}\rangle$, are constructed out of the PS as

$$|\Psi^{(\mathrm{D})}_{k\,M_z - k\,S_eS_h\nu}\rangle = \frac{1}{\sqrt{k!}}\;\hat{k}_-^k\;|\Psi^{(\mathrm{P})}_{k=0\,M_z\,S_eS_h\nu}\rangle\,, \tag{7}$$

where we have used $[\hat{L}_z, \hat{k}_\pm] = \pm\hat{k}_\pm$. In what follows we will often omit the superfluous notation $k = 0$ for the PSs, e.g., $|\Psi^{(\mathrm{P})}_{M_zS_eS_h\nu}\rangle$.

3. Selection Rules for Magneto-Optical Transitions

Selection rules should be formulated in terms of exact quantum numbers. At $B = 0$, the exact quantum numbers can be chosen as the center-of-mass (CM) momentum, a continuous vector $\mathbf{K}$, and the angular momentum projection of the relative motion l_z^{rel}. For simplicity we omit here the spin quantum numbers S_e, S_h and do not discuss the usual spin selection rules. There are two independent optical selection rules associated with the orbital motion: (i) in the dipole approximation, when the photon momentum can be neglected, $\mathbf{K}$ is conserved, and (ii) l_z^{rel} changes according to the polarization of the photon and the process involved.

For charged complexes in B, the quantum number associated with the translational invariance, k, becomes discrete. It is conserved in the dipole approximation [36]. Physically this means that the centers-of-rotation of charged complexes in B in the initial and final states must coincide. (Naturally, the emission or absorption of the photon does not change the total charge of the system.) Because of the coupling of the CM and internal motions for the e–h complexes in B, there is some fundamental difference in the optical selection rules. Note first that neither l_z^{rel}, nor the CM angular momentum projection l_z^{cm}, is separately conserved in B. Only their sum, the total $M_z = l_z^{\mathrm{rel}} + l_z^{\mathrm{cm}}$, is conserved [34]. The second selection rule is formulated, therefore, in terms of M_z.

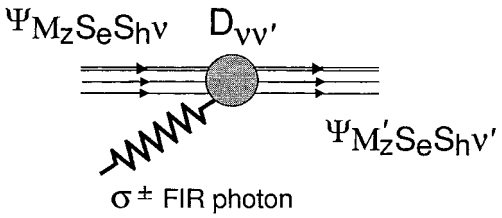

Fig. 1. Intraband absorption processes involving the 2e–h states. The exact selection rule is $M_z' - M_z = \pm 1$ for the $\sigma^{\pm}$ polarization; spin is conserved

Importantly, the two selection rules *cannot be satisfied independently* in B. Indeed, conservation of k implies that the PSs, as having the same $k = 0$, must be directly connected by the optical transition. However, each PS has some specific value of M_z, which is determined by the particulars of interactions. The existence of degenerate daughter states does not bring any freedom, because in each family the quantum numbers k and M_z are connected uniquely via Eq. (7). As a result, transitions between certain families of states turn out to be prohibited (see below); we call such states *dark*. The existence of dark states remains hidden in other (e.g., Landau) gauges (see Appendix).

3.1 Internal intraband transitions

The Hamiltonian describing the interaction with radiation of polarization $\sigma^{\pm}$ and frequency ω in the Faraday geometry is [38]

$$\hat{V}^{\pm} = \sum_j \frac{e_j \mathcal{F}_0 \pi_j^{\pm}}{m_j \omega} \, \mathrm{e}^{-i\omega t} , \tag{8}$$

where $\pi_j^{\pm} = \pi_{jx} \pm i\pi_{jy}$, and $\mathcal{F}_0$ is the electric field amplitude. Since $[\hat{V}^{\pm}, \hat{\mathbf{K}}] = [\hat{V}^{\pm}, \hat{\mathbf{K}}^2] = 0$, the quantum number k is conserved in intraband transitions [32, 35, 36]. This means that the transitions must be allowed directly between the PSs: $|\Psi^{(\mathrm{P})}_{M_z \nu}\rangle \to |\Psi^{(\mathrm{P})}_{M_z' \nu'}\rangle$. Therefore, the PSs must satisfy in the $\sigma^{\pm}$ polarization the usual selection rules $M_z' = M_z \pm 1$, spin conserved (see Fig. 1). For the transition dipole matrix element between the daughter states in the k-th and k'-th generations we have from (7)

$$\begin{aligned} D_{\nu'\nu} &= \langle \Psi^{(\mathrm{D})}_{k' M_z - k' \nu'} | \, \hat{V}^{\pm} | \, \Psi^{(\mathrm{D})}_{k M_z - k \nu} \rangle = \frac{1}{\sqrt{k!k'!}} \, \langle \Psi^{(\mathrm{P})}_{M_z' \nu'} | \, \hat{k}_+^{k'} \hat{V}^{\pm} \hat{k}_-^{k} \, | \Psi^{(\mathrm{P})}_{M_z \nu} \rangle \\ &= \delta_{k,k'} \langle \Psi^{(\mathrm{P})}_{M_z' \nu'} | \, \hat{V}^{\pm} \, | \Psi^{(\mathrm{P})}_{M_z \nu} \rangle \sim \delta_{M_z' \pm 1, M_z} . \end{aligned} \tag{9}$$

Here we have used $[\hat{V}^{\pm}, \hat{k}_-] = [\hat{V}^{\pm}, \hat{k}_+] = 0$ and the operator algebra $[\hat{k}_+, \hat{k}_-] = 1$. We see that $D_{\nu'\nu}$ is the same in all generations. Therefore, $D_{\nu'\nu}$ is a characteristic of the two *families* of states.

3.2 Interband transitions

The interaction of an e–h system with the radiation field with e–h pair annihilation is described by the luminescence operator $\hat{\mathcal{L}}_{\mathrm{PL}} = p_{\mathrm{cv}} \int \mathrm{d}\mathbf{r} \, \hat{\Psi}_{\mathrm{e}}(\mathbf{r}) \, \hat{\Psi}_{\mathrm{h}}(\mathbf{r})$, where p_{cv} is the interband momentum matrix element (see Fig. 2). Consider the photoluminescence (PL) transition $\mathrm{X}^- \to \mathrm{e}_n^- +$ photon, in which an e–h pair is annihilated and an electron is left in the final state in the n-th LL. In PL from the X^- ground state, $n = 1, 2, \ldots$ correspond to so-called shake-up processes (see, e.g. [9, 39] and references therein).

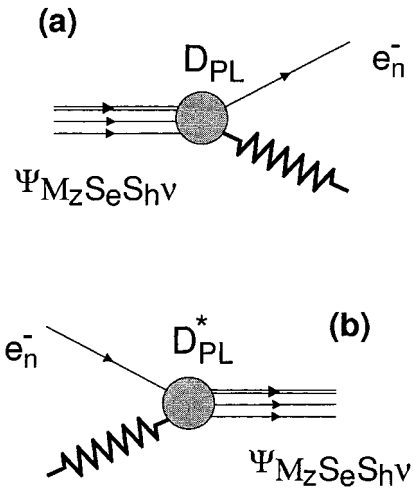

Fig. 2. a) Interband PL process from the 2e–h state. b) Interband absorption process involving electrons in the n-th LL. For a) and b) the exact selection rule is $n = M_z$

The corresponding dipole transition matrix element (Fig. 2a) is $D_{\mathrm{PL}}(\nu) = \langle \phi^{(\mathrm{e})}_{nm} | \hat{\mathcal{L}}_{\mathrm{PL}} | \Psi^{(\mathrm{D})}_{k\, M_z - k\, \nu} \rangle$. Here $|\phi^{(\mathrm{e})}_{nm}\rangle$ is the factored wave function of the electron in the $n = 0, 1, \ldots$ LL with the oscillator quantum number $m = 0, 1, \ldots$ (see, e.g. [33, 34, 37]). The latter is the single-particle analog of the quantum number k in (7). The angular momentum projection $m_z = n - m$. Due to the change of the Bloch parts of orbital wave functions in this case, the usual selection rule $\Delta M_z = 0$ holds for the envelope functions. Thus, $m_z = n - m = M_z - k$ must hold. Because of the commutativity $[\hat{\mathcal{L}}_{\mathrm{PL}}, \hat{\mathbf{K}}] = 0$, the oscillator quantum number should be conserved: $m = k$. We see, therefore, that [36]

$$D_{\mathrm{PL}}(\nu) \sim \delta_{n, M_z} \,. \tag{10}$$

This is an important result. It shows that the X^- PL transition is only possible when the electron is left in a single and specific electron LL with the number $n = M_z$; M_z here is the angular momentum projection of the PS. The implications for *any* isolated X^- state in a translationally invariant system in B are:

– X^- states with $M_z < 0$ are *dark* in PL;

– X^- shake-up processes in PL are strictly prohibited. (For donor-bound X^- states in zero LLs with $M_z > 0$ (which are energetically favorable), the optical transitions are allowed *only* via shake-up processes (see [18])).

The general exact selection rules discussed in this section are applied in the following to describe the magneto-optical transitions of the 2D charged MXs X^-.

4. 2D Trions in Zero and Higher Landau Levels

In the limit of high magnetic fields such that [15, 16, 36]

$$\hbar\omega_{\mathrm{ce(h)}} = \frac{\hbar e B}{m_{\mathrm{e(h)}}} \gg E_0 = \sqrt{\frac{\pi}{2}}\, \frac{e^2}{\epsilon l_B} \,, \tag{11}$$

LLs remain well-defined. In this limit the three-particle 2e–h states can be labeled in the first approximation as $|\Psi^{(n_{\mathrm{e}} n_{\mathrm{h}})}_{k\, M_z\, S_{\mathrm{e}} S_{\mathrm{h}} \nu}\rangle$. Here, in addition to the exact quantum numbers (4), a pair of quantum numbers $(n_{\mathrm{e}} n_{\mathrm{h}})$ has been introduced, describing the total electron LL number n_{e} and the hole LL number n_{h} [37]. The expansion in LLs for charged e–h complexes that preserves all symmetries requires summing over an infinite number of e- and h-states in zero LLs. The method has been described elsewhere [37].

4.1 Eigenstates

The calculated 2e–h eigenspectra in several of the lowest LLs $(n_{\mathrm{e}} n_{\mathrm{h}})$ are presented in Figs. 3–5. Note that only the PSs $k = 0$ states are shown. Filled dots above free LLs in

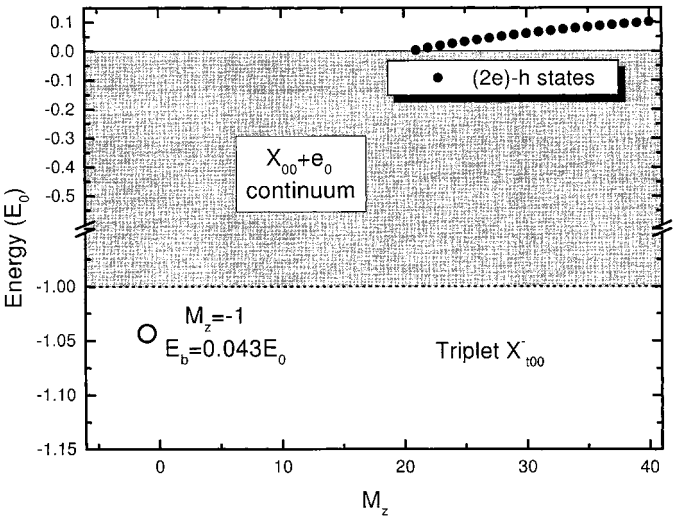

Fig. 3. Eigenspectra of the three-particle 2e–h electron triplet $S_e = 1$ states in zero LLs $(n_e n_h) = (00)$. Only states with $k = 0$ are shown. Energy is given relative to that of free LLs $\frac{1}{2}\hbar(\omega_{ce} + \omega_{ch})$, in units of $E_0 = \sqrt{\pi/2}\, e^2/\epsilon l_B$

Figs. 3–5 show positions of the excited three-particle states, denoted as (2e)–h. These states originate from the excited states of two electrons that are bound in 2D: despite the e–e repulsion, their relative motion is finite because of the confining effect of the magnetic field [40]. Our results show that an infinite number of such states remain bound in the presence of the hole. For $M_z \gg 1$, the hole can be at a sufficiently large distance from two electrons so as not to perturb strongly their relative motion. In this situation, the relative motion of two electrons can be approximately described by the

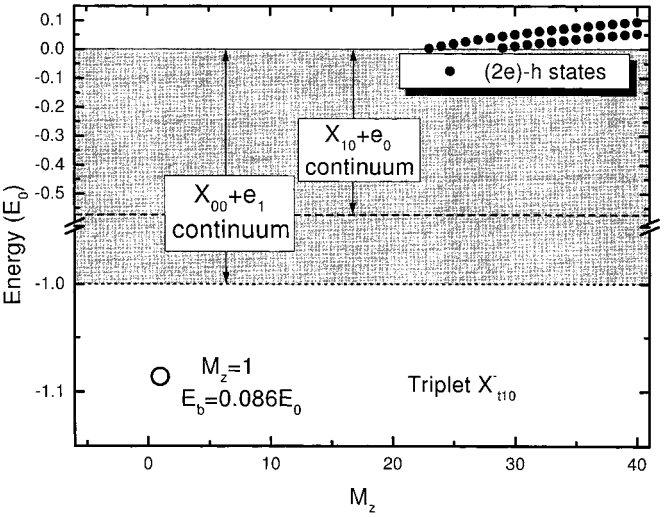

Fig. 4. Same as in Fig. 1 for states in the $(n_e n_h) = (10)$ LLs. Energy is given relative to $\hbar(\frac{3}{2}\,\omega_{ce} + \frac{1}{2}\,\omega_{ch})$

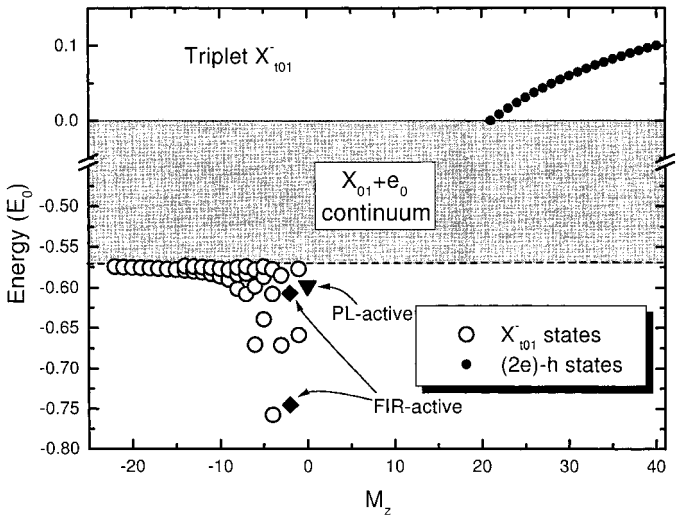

Fig. 5. Same as in Fig. 1 for states in the $(n_e n_h) = (01)$ LLs. Energy is given relative to $\hbar(\frac{1}{2}\,\omega_{ce} + \frac{3}{2}\,\omega_{ch})$. The solid triangle marks the state with $M_z = 0$ that may undergo a weak interband PL transition $X^-_{t01} \to e^-_0 +$ photon. The solid diamonds mark the final states in the intraband internal inter-LL transitions $X^-_{t00} \to X^-_{t01}$, which are strong in the σ^- polarization

relative e–e angular momentum projection m. The larger m, the larger is the e–e distance. With increasing M_z channels with larger m appear as the bound (2e)–h states. In Figs. 3 and 5, for instance, only one such family (with $m = 1$) has developed; states with even $m = 0, 2, \ldots$ are forbidden for electron triplets in the zero electron LL. Asymptotically ($M_z \to \infty$) an infinite number of different (2e)–h families appear in the spectra. The bound discrete (2e)–h states form therefore rather dense spectra, a quasi-continuum. The hole is at a finite distance from the electrons in these states: the relative motions of all three particles are finite. In an approach that fails to recognize different k-states, it would have been hardly possible to identify the nature of the excited discrete states above free LLs. Note that bound excited states of a similar nature exist in the spectra of the 2D negative donor ion D^- in strong magnetic fields [28].

The shaded areas in Figs. 3–5 correspond to the *three-particle continuum*. It is formed by the neutral MX, *all* states of which have bound internal and extended CM motions [18, 41], and an electron in a scattering state. The electron is on average at infinity (see footnote [2])) from the MX: the mean quantum mechanical distance between, e.g., two electrons is infinite in any scattering state, $\sqrt{\langle(\mathbf{r}_1 - \mathbf{r}_2)^2\rangle_{sc}} = \infty$. For the $(n_e n_h) = (10)$ LLs, there are two different overlapping MX bands (see Fig. 4). One corresponds to the X_{00} MX (e and h in their zero LLs) with the second electron in a scattering state in the first LL. The lower continuum edge lies at the ground state energy $-E_0$ of the X_{00} MX [41]. The second, narrow continuum corresponds to the X_{10} MX (e in the first and h in the zero LL). The lower continuum edge lies at the ground state energy $-0.574E_0$ of the X_{10} MX. For the isolated MX, it is achieved at a finite momentum $\mathbf{K}l_B \simeq 1.19$; an inverse square-root van Hove singularity in the X_{10} density of states is associated with this extremum in 2D. There is another extremum [41] in the X_{10} dispersion at $\mathbf{K} = 0$ producing a finite jump in the X_{10} density of states at an energy $-0.5E_0$. For the

$(n_e n_h) = (01)$ LLs, there is only one continuum formed by the X_{01} MX in the zero electron and first hole LLs (Fig. 4). The spectra of the isolated X_{01} and X_{10} neutral MXs are equivalent.

There is a number of low-lying bound X^- states. In the zero LLs, there is only one bound state, the triplet X_{t00} with a small binding energy $0.044E_0$ (counted from the lower continuum edge, see Fig. 3) [15, 16, 36]. In the 2D system in the high-B limit, there are no bound singlet X^- states in the zero LLs. This is in contrast to the situation at $B = 0$, where only the singlet X^- binds, and to quasi-2D systems at finite B, where both singlet and triplet X^- states are bound [16]. In the next electron LL $(n_e n_h) = (10)$, there is also only one bound state, which is the triplet X^-_{t10} with larger binding energy $0.086E_0$ [36, 37]. This resembles a stronger binding of the triplet donor ion D^- in the first electron LL and has the same physical origin, which is discussed in [28, 36]. In the next hole LL $(n_e n_h) = (01)$, there are *many* bound states, both triplets X^-_{t01} (Fig. 5) and singlets X^-_{s01}; spectra for the latter have been presented elsewhere [37]. This is explained by the fact that the neutral X_{01} MX is relatively weakly bound, so that many bound X^- states split off from the corresponding narrow continuum. The ground triplet X^-_{t01} state has $M_z = -4$ and rather large binding energy $0.184E_0$. For the singlet X^-_{s01} ground state the corresponding values are $M_z = -3$ and $0.207E_0$ [37].

4.2 Interband transitions

The spectra obtained for the X^- eigenstates, together with the selection rule (12), make it possible to qualitatively understand interband transitions involving both discrete bound X^- states and the continuum. As follows from (12), all 2e–h states that have negative total $M_z < 0$ are dark in PL. An important example is the ground triplet X^-_{t00} state in zero LLs that has $M_z = -1$ (Fig. 3) and is therefore dark [36]. This result has also been found in the spherical geometry [20]. In the strictly-2D high-B limit it also follows [15] from the "hidden symmetry" [42–44] in e–h systems. Importantly, quasi-2D effects, admixture of higher LLs, or a complex character of the valence band [36] will not make the ground X^-_t state bright, as long as it remains at $M_z < 0$. Finite-size calculations performed in the spherical geometry [21] indicate that the second "bright" triplet X^-_{tb} with $M_z = 0$ may exist in quasi-2D systems at finite B. High-accuracy calculations in plane geometries for realistic QW parameters give, however, a rather small binding energy (0.15 ± 0.1) meV for wide 300 Å GaAs QWs at high B and indicate that this state is unbound in 100 Å QWs.

Let us now consider bound states in higher LLs. The strongly bound triplet X^-_{t10} state in the first electron LL (10) has $M_z = 1$ (Fig. 4). It is PL active only in the process $X^-_{t10} \rightarrow e^-_1 +$ photon, which leaves the electron in the first LL. This PL process has a large dipole transition matrix element. Consider now the *absorption* (Fig. 2b) involving the low-density 2DEG in the zero LL with final states belonging to the first electron LL. Such absorption processes were observed [45] in the low-density 2DEG in magnetic fields and called a *"Combined Exciton-Cyclotron Resonance"* (ExCR). Due to the selection rule (10), the transitions to the bound triplet state $e^-_0 + \text{photon} \rightarrow X^-_{t10}$ and transitions to the excited bound states (2e)–h are prohibited. Therefore, when the final states belong to the first electron LL, the ExCR processes can only go via transitions to the *continuum*. There are two overlapping continua in the (10) LL (Fig. 4). Somewhat surprisingly, theory [46] predicts that both channels $e^-_0 + \text{photon} \rightarrow X_{00} + e^-_1$ and

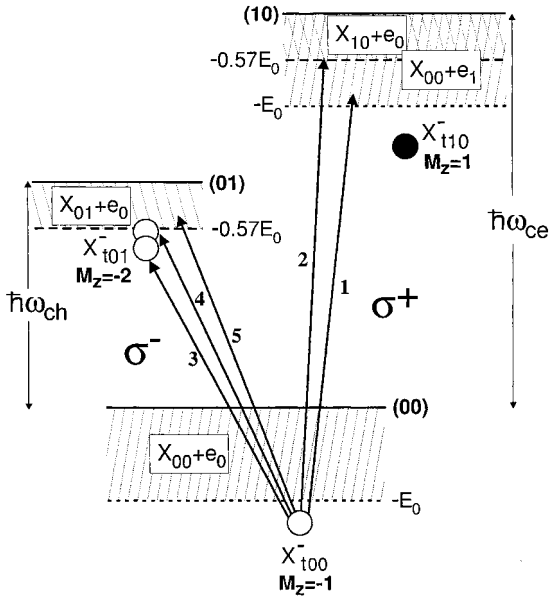

Fig. 6. Schematic drawing of the 2e–h triplet $S_e = 1$ eigenstates in zero and two higher LLs relevant for the inter-LL transitions from the triplet ground state in the $\sigma^{\pm}$ polarizations

$e_0^- + \text{photon} \rightarrow X_{10} + e_0^-$ have large oscillator strengths. Therefore, the high-field ExCR should have a double-peak structure.

4.3 Intraband transitions

Consider the inter-LL transitions from the 2D triplet X^-_{t00} ground state. In principle, both bound-to-bound and photoionizing bound-to-continuum transitions are possible in B. This is in contrast to the 2D negative donor ion D^-, for which all internal transitions are bound-to-bound, and there are no allowed photoionizing transitions in strong magnetic fields [27, 28]. In the σ^+ (σ^-) polarization the inter-LL e-CR-like $\Delta n_e = 1$ (h-CR-like $\Delta n_h = 1$) transitions are strong and gain strength with B (Fig. 6). All other transitions are only due to LL mixing and are weak; transition matrix elements $\sim [E_0/\hbar\omega_{ce(h)}]^2 \sim B^{-1}$. The transitions must simultaneously satisfy the two selection rules (11): $\Delta k = 0$ and $\Delta M_z = \pm 1$.

Consider first the σ^+ polarization. Because of the selection rules, the bound-to-bound $X^-_{t00} \rightarrow X^-_{t10}$ transition, which lies below the e-CR, is strictly prohibited in a translationally invariant system [36]. There are two channels of photoionizing transitions to the continuum: $X^-_{t00} + \text{photon} \rightarrow X_{00} + e_1^-$ and $X^-_{t00} + \text{photon} \rightarrow X_{10} + e_0^-$, shown as transitions 1 and 2 in Fig. 6. Both have large oscillator strengths and intrinsic linewidths $\sim 0.2E_0$. The situation resembles the ExCR transitions discussed above. The corresponding double-peak structure in the singlet and triplet X^- inter-LL transitions has been observed experimentally [14].

In the σ^- polarization, there are two bound-to-bound [35] $X^-_{t00} \rightarrow X^-_{t01}$ transitions with final states having $M_z = -2$ (transitions 3 and 4 in Fig. 6). Both transitions lie above the h-CR. There is also a broad photoionizing transition 5 to the $X_{01} + e_0$ continuum. Note that transitions to many families of the bound X^-_{t01} states (see Fig. 5) are forbidden in a translationally invariant system. As the presence of disorder would make many of these transitions partly allowed, the spectra are expected to be sample dependent.

5. Many-Body Effects in Internal Transitions of Charged Magnetoexcitons

5.1 Experiment

Optically detected resonance (ODR) spectroscopy combines visible/near-infrared photoluminescence (PL) with far-infrared (FIR) methods [47]: one monitors the changes in

the intensity and shape of the PL signal of a sample that are induced by the (resonant) absorption of radiation from a FIR laser. The sample is mounted inside a variable temperature insert in a liquid helium cryostat at the center of a superconducting magnet and is kept at low temperatures, typically 4.2 K. The external magnetic field (up to 15 T) is used to tune the various FIR transitions into resonance with the FIR laser photon energy, which ranges from 2.87 to 17.6 meV. Optical fibers are used to transport the exciting light and collect the PL signal, and a light pipe and condensing light cone system is used to guide and focus the FIR radiation to the sample inside the cryostat. The light intensity of the HeNe or Ar^+ ion excitation lasers is approximately 500 mW/cm^2, and the power of the FIR laser at the output coupler of the laser head lies between 20 and 80 mW. The FIR radiation is modulated with an external chopper at a frequency of approximately 200 Hz, and phase-sensitive, lock-in techniques are used to detect the induced changes in the PL signal, which are typically between 0.1 and 10% of the PL intensity.

Three GaAs/$Al_{0.3}Ga_{0.7}$As multiple quantum well samples, modulation-doped with silicon in the barriers, were studied. The structures of these low, medium, and high carrier density samples are [(*well/barrier–thickness* in Å) × *repetitions*]: sample 1: (200/400) × 40; sample 2: (240/480) × 20; and sample 3: (240/240) × 10.

Figure 7 shows ODR scans for all three samples taken at a FIR laser photon energy of 12.8 meV. In addition, the magnetic fields corresponding to electron filling factor $\nu_e = 2$, $B = 0.4$, 1.7, and 4.0 T, respectively, (determined by magneto-photoluminescence measurements) are indicated by the downward pointing arrows. The position of electron cyclotron resonance, present in all three traces, is marked by the vertical solid line at $B = 7.7$ T labeled e-CR. A second feature marked by the upward pointing arrow is observed at magnetic fields just below e-CR. It is identified as the triplet-like internal transition of X^- [14, 36]. As the carrier density is increased (following the traces from top to bottom), this feature evolves from a shoulder to e-CR in the low density sample to a clear peak in the high density sample as it moves to lower magnetic fields and therefore experiences a *blue-shift* in energy. Other resonances observed at lower magnetic fields are identified as the internal singlet-like transitions of X^- [14, 36].

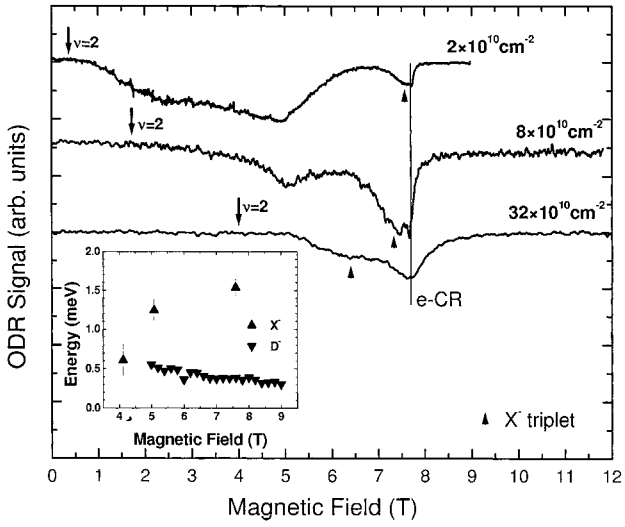

Fig. 7. ODR spectra of samples 1, 2, and 3, recorded for a FIR laser photon energy of 12.8 meV. The position of the e-CR is indicated by the solid vertical line, the triplet-like X^- transition is marked by the upright arrows, and filling factor $\nu_e = 2$ is indicated for each sample by the downward pointing arrows. Inset: comparison of the blue-shift of X^- and D^- plotted as a function of magnetic field (see text for details)

They are most notable in the low and medium density samples, but are not seen in the most heavily doped sample for which they would occur at fields below that corresponding to $\nu_e = 2$. This behavior is not the subject of the present discussion.

The inset to Fig. 7 shows that the experimentally observed blue-shift of the dominant internal X^- transition extracted from the low and medium density samples is larger than the corresponding singlet-like transition of D^- measured in a well- and barrier-doped GaAs multiple quantum-well (MQW) sample of similar dimensions and carrier concentration [48, 49].

5.2 Theory

To understand the experimental findings, we consider intraband excitations from the ground state of the 2D system with integer fillings of electron LLs $\nu_e = 2\pi l_B^2 n_e = 1, 2$ containing a low-density gas of photoexcited mobile valence band holes (see Section 5.1). The collective excitations correspond to transitions to the correlated e–h final state. It can be viewed as an interacting few-particle system: The final state consists of the conduction band electron in the empty $n = 1$ LL, e_{cb1}, a conduction band hole in an otherwise filled $n = 0$ LL, h_{cb0}, and a mobile valence band hole in the $n = 0$ LL, h_{vb0}. Similar ideas have been exploited for a description of the interband PL from the 2DEG in high fields (see [50] and references therein to earlier work). Notice now that we can treat the final state as a positively charged complex X^+, with a strong exchange interaction between the particles e_{cb1} and h_{cb0}. The intraband optical transition matrix element (Fig. 8a) resembles an interband transition (Fig. 2b). Classification of states and optical selection rules can therefore be formulated following the recipes of Sections 2 and 3.

In the absence of the valence band hole, the intraband collective excitations are charge-neutral 2D magnetoplasmons [40, 51]. They are characterized by the conserved CM momentum **K**, have finite relative motion (a bound e_{cb1}–h_{cb0} pair) and extended CM motion. Only $\mathbf{K} = 0$ magnetoplasmons are e-CR active and, due to Kohn's theorem [38], have the bare cyclotron energy $\hbar\omega_{ce}$. Magnetoplasmons with $\mathbf{K} \neq 0$ form at $\nu_e = 1$ a band of finite width $E_0/2$. In the presence of the valence band hole, different **K** states are admixed into the three-particle X^+ eigenstate. Kohn's theorem is no longer applicable, and many states acquire oscillator strength.

Calculations of the eigenspectra of the three-particle 2h–e excitations and matrix elements of intraband optical transitions $h_{vb0} + \text{photon} \rightarrow 2h\text{–}e$ (Fig. 8) were performed using a method that is similar to our

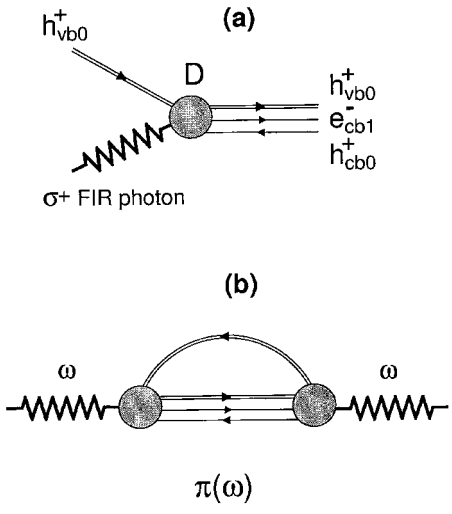

Fig. 8. a) Intraband absorption processes involving the valence band hole h_{vb0} in the initial state and 2e–h final states. b) Polarization operator $\pi(\omega)$ describing intraband absorption in the 2DEG with integer filling of LLs in the presence of the valence band hole. Absorption $-2\,\mathrm{Im}\,\pi(\omega) \sim n_h$, where n_h is the density of holes

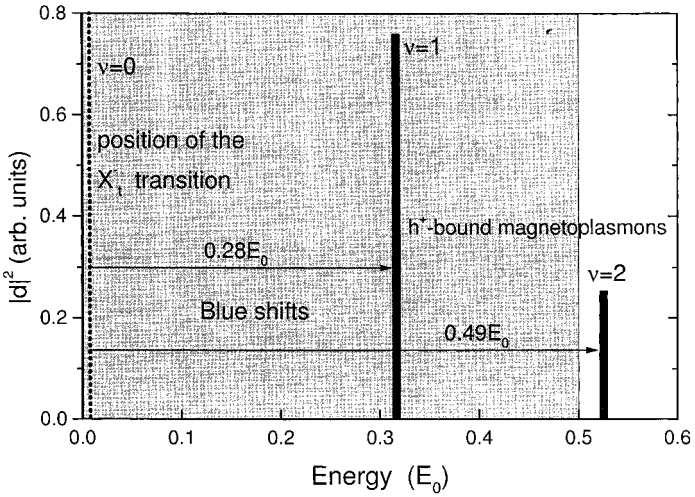

Fig. 9. Energies and oscillator strengths of the collective modes, magnetoplasmons bound to the mobile valence hole, for electron filling factors $\nu_e = 1, 2$. They are blue-shifted relative to the internal transition of the isolated ($\nu \to 0$) triplet charged MX X^-. The shaded area shows the position of the magnetoplasmon continuum

treatment of the X^- states [36, 37]; a detailed account will be presented elsewhere. Here we discuss the spectra of transitions that have energies larger than the e-CR energy $\hbar\omega_{ce}$. For electron filling factor $\nu_e = 1$, there exists one rather sharp peak. It corresponds to the optically active 2h–e state, a three-particle resonance that lies within the magnetoplasmon continuum (Fig. 9). With increasing ν_e, exchange-correlation effects are enhanced. As a result, the quasi-bound three-particle state shifts upward in energy. For filling factor $\nu_e = 2$ it moves out of the continuum and becomes a truly bound 2h–e state that is characterized by finite relative motions of all particles. For both $\nu_e = 1$ and 2, the optically active state describes a magnetoplasmon bound to the mobile valence band hole h_{vb0}. Note that with the increased energy separation from the optically-active e-CR mode, this state loses oscillator strength.

The energies of collective excitations are larger than the energy of the internal transition [14, 36] of the isolated ($\nu_e \to 0$) triplet X^- state. This means that X^- transitions are blue-shifted in the presence of excess electrons. The calculated blue-shifts of the X^-–triplet at $\nu_e = 1$ and $\nu_e = 2$ are $0.28E_0$ and $0.49E_0$, respectively. This behavior resembles the blue-shift of the two-electron negative donor center D^- in the presence of excess electrons [48, 49], which is understood in terms of magnetoplasmons localized on fixed donor ions D^+ [52, 53]. In the latter case the translational invariance is broken by the donor potential and classification of states is qualitatively different. Quantitatively, the blue-shifts of the X^- and D^- are comparable; for the latter they are given by $0.15E_0$ and $0.34E_0$ at $\nu_e = 1$ and 2, respectively [52]. In agreement with experiment, the predicted blue-shift of the X^- is larger than that of the D^- (see inset to Fig. 7).

6. Conclusions

Exact optical selection rules for inter- and intra-band transitions of charged e–h complexes in magnetic fields have been discussed. We have considered in detail the struc-

ture of the 2D X^- eigenspectra in several LLs. It has been shown that generally there exists a multitude of discrete bound X^- states, both singlets and triplets, associated with higher LLs. Only few of these states are optically active in a translationally invariant system in a magnetic field.

The effect of excess electrons on internal transitions of charged MXs X^- in quantum wells has been studied experimentally and theoretically. The observed blue shift is explained in terms of a new type of collective excitations, magnetoplasmons bound to a mobile valence hole.

Acknowledgements We are grateful to A. Yu. Sivachenko and D. R. Yakovlev for many interesting discussions. We thank W. Schaff for the excellent MBE growth of the GaAs samples used in this study. This work was supported in part by NSF grant DMR 9722625, by COBASE grant R175, and by the Russian Ministry of Science program "Nanostructures". A. B. D. acknowledges support of the Humboldt Foundation.

Appendix

In the Landau gauge, translational invariance is manifestly preserved in one direction [54]. It might seem that the implications due to the magnetic translations could be more transparent in this gauge. Here we show that for charged e–h complexes this is not the case: the existence of dark states remains in fact hidden in the Landau gauge. Fundamentally, this happens because in the Landau gauge the rotational symmetry of *space* is manifestly broken in the *Hamiltonian*. The choice of the symmetric gauge leaves both dynamical symmetries, rotations about the **B** axis, and the magnetic translations, intact.

The transformation from the symmetric $\mathbf{A}(\mathbf{r}) = \mathbf{B} \times \mathbf{r}/2$ to the Landau gauge $\mathbf{A}'(\mathbf{r}) = (0, Bx, 0) = \mathbf{A}(\mathbf{r}) + \nabla f(\mathbf{r})$, where $f(\mathbf{r}) = Bxy/2$, is realized with the help of the unitary operator $\hat{U} = \exp\left(i \sum_j e_j B f(\mathbf{r}_j)/\hbar c\right)$ [54]. The eigenstates and operators in the Landau gauge will be denoted below by the tilde sign. As an example, the exact charged degenerate eigenstate in the ν-th family with a 1D momentum k_y is designated as $|\tilde{\Psi}_{k_y\nu}\rangle$. The spin quantum numbers are omitted for brevity (cf. (7)). Consider in the Landau gauge the dipole transition matrix elements, analogous to Eq. (9), between the states from the ν-th and ν'-th families. The operator of the interaction with the radiation of polarization $\sigma^{\pm}$ (8) is $\tilde{V}^{\pm} = \hat{U} V^{\pm} \hat{U}^{\dagger}$ in this gauge. It conserves k_y, therefore $\langle \tilde{\Psi}_{k_y\nu} | \tilde{V}^{\pm} | \tilde{\Psi}_{k'_y\nu'} \rangle \sim \delta(k_y - k'_y)$. Also, $\tilde{D}_{\nu\nu'}(k_y) \equiv \langle \tilde{\Psi}_{k_y\nu} | \tilde{V}^{\pm} | \tilde{\Psi}_{k_y\nu'} \rangle$ does not depend on k_y. Indeed, a state with some arbitrary k'_y, $|\tilde{\Psi}_{k'_y\nu}\rangle$, can be constructed from any other state in the same ν-th family, $|\Psi_{k_y\nu}\rangle$, with the help of the unitary operator of *translations in the momentum* k_y space, $\hat{T}_{k_y}$,

$$|\Psi_{k'_y\nu}\rangle = \hat{T}_{k'_y - k_y} |\Psi_{k_y\nu}\rangle , \tag{A1}$$

$$\hat{T}_{k_y} = \exp\left(-i\hat{\tilde{K}}_x k_y / l_B^2\right) . \tag{A2}$$

This follows from the (gauge independent) commutation relation for the x- and y-components of the operator of the magnetic translations $[\hat{\tilde{K}}_x, \hat{\tilde{K}}_y] = i l_B^{-2}$ and from the commutativity of $\hat{\tilde{\mathbf{K}}}$ with the Hamiltonian, $[\tilde{H}, \hat{\tilde{\mathbf{K}}}] = 0$. Since $[\hat{T}_{k_y}, \tilde{V}^{\pm}] = [\hat{T}^{\dagger}_{k_y}, \tilde{V}^{\pm}] = 0$, we

have

$$\tilde{D}_{\nu\nu'}(k_y') = \langle \tilde{\Psi}_{k_y'\nu} |\, \tilde{V}^{\pm} \,| \tilde{\Psi}_{k_y'\nu'} \rangle = \langle \tilde{\Psi}_{k_y\nu} |\, \hat{T}^{\dagger}_{k_y'-k_y} \tilde{V}^{\pm} \hat{T}_{k_y'-k_y} \,| \tilde{\Psi}_{k_y\nu'} \rangle$$
$$= \langle \tilde{\Psi}_{k_y\nu} |\, \tilde{V}^{\pm} \,| \tilde{\Psi}_{k_y\nu'} \rangle = \tilde{D}_{\nu\nu'}(k_y)\,. \tag{A3}$$

However, unlike the situation in the symmetric gauge, *there are no* PSs in the Landau gauge: states with arbitrary k_y are allowed. Therefore, we cannot proceed here as in Eq. (9). As a result, the fact that some of the families of states are dark turns out to be hidden in the Landau gauge. To make it apparent, one has to go back to the symmetric gauge

$$|\tilde{\Psi}_{k_y\nu}\rangle = \sum_{k=0}^{\infty} \alpha_{k_y}^{(\nu)}(k)\, \hat{U} \frac{1}{\sqrt{k!}}\, \hat{k}_-^k \,|\Psi_{M_z\nu}^{(\mathrm{P})}\rangle\,, \tag{A4}$$

where $\alpha_{k_y}^{(\nu)}(k)$ are expansion coefficients, and we have used Eq. (7). Then, using (9) yields

$$\tilde{D}_{\nu\nu'}(k_y) = \left[\sum_{k=0}^{\infty} \alpha_{k_y}^{(\nu)}(k)^*\, \alpha_{k_y}^{(\nu')}(k)\right] D_{\nu\nu'} = D_{\nu\nu'}\,, \tag{A5}$$

where we have used the fact that $\sum_{k=0}^{\infty} \alpha_{k_y}^{(\nu)}(k)^*\, \alpha_{k_y}^{(\nu')}(k) = 1$ for arbitrary families ν, ν'. This fact can be established by group-theoretical considerations [31]. It physically follows also from, e.g., the sum rule for the oscillator strengths and the fact that $\tilde{D}_{\nu\nu'}$ does not depend on k_y. Above we have not used a concrete form of the gauge transformation $\hat{U}$. Therefore, we have proved that the dipole transition matrix element $D_{\nu\nu'}$ – a characteristic of two macroscopically degenerate families of charged states – is gauge-invariant, as it should be.

References

[1] M. A. LAMPERT, Phys. Rev. Lett. **1**, 450 (1958).
[2] B. STEBE and A. AINANE, Superlattices Microstruct. **5**, 545 (1989).
[3] C. RIVA, F. M. PEETERS, and K. VARGA, phys. stat. sol. (a) **178**, 513 (2000); Phys. Rev. B **61**, 13873 (2000).
[4] A. ESSER, E. RUNGE, R. ZIMMERMANN, and W. LANGBEIN, Phys. Rev. B **62**, 8232 (2000).
[5] K. KHENG, R. T. COX, Y. MERLE D'AUBIGNE, F. BASSANI, K. SAMINADAYAR, and S. TATARENKO, Phys. Rev. Lett. **71**, 1752 (1993).
[6] G. FINKELSTEIN, H. SHTRIKMAN, and I. BAR-JOSEPH, Phys. Rev. Lett. **74**, 976 (1995); Phys. Rev. B **53**, R1709 (1996); S. GLASBERG, G. FINKELSTEIN, H. SHTRIKMAN, and I. BAR-JOSEPH, Phys. Rev. B **59**, R10425 (1999).
[7] A. J. SHIELDS, M. PEPPER, M. Y. SIMMONS, and D. A. RITCHIE, Phys. Rev. B **52**, 7841 (1995).
[8] D. GEKHTMAN, E. COHEN, ARZA RON, and L. N. PFEIFFER, Phys. Rev. B **54**, 10320 (1996).
[9] O. V. VOLKOV, V. E. ZHITOMIRSKII, I. V. KUKUSHKIN, K. VON KLITZING, and K. EBERL, J. Exp. Theor. Phys. Lett. **67**, 744 (1998).
[10] H. OKAMURA, D. HEIMAN, M. SUNDARAM, and A. C. GOSSARD, Phys. Rev. B **58**, R15985 (1998).
[11] M. HAYNE, C. L. JONES, R. BOGAERTS, C. RIVA, A. USHER, F. M. PEETERS, F. HERLACH, V. V. MOSHCHALKOV, and M. HENINI, Phys. Rev. B **59**, 2927 (1999).
[12] G. V. ASTAKHOV, D. R. YAKOVLEV, V. P. KOCHEREshko, W. OSSAU, J. NÜRNBERGER, W. FASCHINGER, and G. LANDWEHR, Phys. Rev. B **60**, R8485 (1999).
[13] G. KIOSEOGLOU, H. D. CHEONG, H. A. NICKEL, A. PETROU, B. D. MCCOMBE, and W. SCHAFF, Phys. Rev. B **61**, 4780 (2000).

[14] H. A. Nickel, G. S. Herold, T. Yeo, G. Kioseoglou, Z. X. Zhiang, B. D. McCombe, A. Petrou, D. Broido, and W. Schaff, phys. stat. sol. (b) **210**, 341 (1998).
A. B. Dzyubenko, A. Yu. Sivachenko, H. A. Nickel, T. M. Yeo, G. Kioseoglou, B. D. McCombe, and A. Petrou, Physica E **6**, 156 (2000).
[15] J. J. Palacios, D. Yoshioka, and A. H. MacDonald, Phys. Rev. B **54**, R2296 (1996).
[16] D. M. Whittaker and A. J. Shields, Phys. Rev. B **56**, 15185 (1997).
[17] C. Riva, F. M. Peeters, and K. Varga, Phys. Rev. B **63**, 115302 (2001).
[18] A. B. Dzyubenko, Phys. Lett. A **173**, 311 (1993).
[19] A. Wójs and P. Hawrylak, Phys. Rev. B **51**, 10880 (1995).
[20] A. Wójs, P. Hawrylak, and J. J. Quinn, Phys. Rev. B **60**, 11661 (1999).
[21] A. Wójs, J. J. Quinn, and P. Hawrylak, Phys. Rev. B **62**, 4630 (2000).
[22] F. D. M. Haldane, Phys. Rev. Lett. **51**, 605 (1983).
[23] B. Stebe, A. Ainane, and F. Dujardin, J. Phys.: Condens. Matter **8**, 5383 (1996).
[24] B. Stebe, E. Feddi, A. Ainane, and F. Dujardin, Phys. Rev. B **58**, 9926 (1998).
[25] H. A. Bethe and E. E. Salpeter, Quantum Mechanics of One- and Two-Electron Atoms, Springer-Verlag, Berlin 1957.
[26] S. Huant, S. P. Najda, and B. Etienne, Phys. Rev. Lett. **65**, 1486 (1990).
[27] D. M. Larsen and S. Y. McCann, Phys. Rev. B **45**, 3485 (1992).
[28] A. B. Dzyubenko, Phys. Lett. A **165**, 357 (1992).
[29] A. B. Dzyubenko and A. Yu. Sivachenko, Phys. Rev. B **48**, 14690 (1993).
[30] R. S. Ryu, Z. X. Jiang, W. J. Li, B. D. McCombe, and W. Schaff, Phys. Rev. B **54**, R11086 (1996).
[31] E. Brown, in: Solid State Physics, Vol. 22, Eds. E. Ehrenreich and F. Seitz, Academic Press, New York 1968.
[32] J. E. Avron, I. W. Herbst, and B. Simon, Ann. Phys. (USA) **114**, 431 (1978).
[33] Z. F. Ezawa, Quantum Hall Effects, World Scientific Publ. Co., Singapore 2000.
[34] B. R. Johnson, J. O. Hirschfelder, and K. H. Yang, Rev. Mod. Phys. **55**, 109 (1983).
[35] A. B. Dzyubenko and A. Yu. Sivachenko, J. Exper. Theor. Phys. Lett. **70**, 514 (1999).
[36] A. B. Dzyubenko and A. Yu. Sivachenko, Physica E **6**, 226 (2000);
Phys. Rev. Lett. **84**, 4429 (2000).
[37] A. B. Dzyubenko, Solid State Commun. **113**, 683 (2000);
cond-mat/0107611.
[38] W. Kohn, Phys. Rev. **123**, 1242 (1961).
[39] G. Finkelstein, H. Shtrikman, and I. Bar-Joseph, Phys. Rev. B **53**, 12593 (1996);
56, 10 326 (1997).
[40] Yu. A. Bychkov, S. V. Iordanskii, and G. M. Eliashberg, J. Exper. Theor. Phys. Lett. **33**, 143 (1981).
[41] I. V. Lerner and Yu. E. Lozovik, J. Exper. Theor. Phys. **51**, 588 (1980).
[42] I. V. Lerner and Yu. E. Lozovik, J. Exper. Theor. Phys. **53**, 763 (1981).
[43] A. B. Dzyubenko and Yu. E. Lozovik, Sov. Phys. — Solid State **25**, 874 (1983);
26, 938 (1984);
J. Phys. A **24**, 415 (1991).
[44] A. H. MacDonald and E. H. Rezayi, Phys. Rev. B **42**, 3224 (1990).
[45] D. R. Yakovlev, V. P. Kochereshko, R. A. Suris, H. Schenk, W. Ossau, A. Waag, G. Landwehr, P. C. M. Christianen, and J. C. Maan, Phys. Rev. Lett. **79**, 3974 (1997).
[46] A. B. Dzyubenko, cond-mat/0106229.
[47] G. S. Herold, H. A. Nickel, J. G. Tischler, B. A. Weinstein, and B. D. McCombe, Physica E **2**, 39 (1998).
[48] J.-P. Cheng, Y. J. Wang, B. D. McCombe, and W. Schaff, Phys. Rev. Lett. **70**, 489 (1993).
[49] Z. X. Jiang, B. D. McCombe, J.-L. Zhu, and W. Schaff, Phys. Rev. B **56**, R1692 (1997).
[50] E. I. Rashba and M. D. Sturge, Phys. Rev. B **63**, 045305 (2000).
[51] C. Kallin and B. I. Halperin, Phys. Rev. B **30**, 5655 (1984).
[52] A. B. Dzyubenko and A. Yu. Sivachenko, J. Exper. Theor. Phys. Lett. **57**, 507 (1993);
A. B. Dzyubenko and Yu. E. Lozovik, J. Exper. Theor. Phys. **77**, 617 (1993).
[53] P. Hawrylak, Phys. Rev. Lett. **72**, 2943 (1994).
[54] L. D. Landau and E. M. Lifshits, Quantum Mechanics, 3rd ed., Pergamon Press, New York 1977.